RSC Advances

ROYAL SOCIETY OF CHEMISTRY

www.rsc.org/advances

Influence of Less Active Initiator on the Living Performance of Atom Transfer Radical Polymerization and the Structure of Grafted Copolymer Synthesized

Honghong Gong,[a] Junjie Li,[a] Daming Di,[b] Na Li[b] and Zhicheng Zhang*[a]

Graphical Abstract

By monitoring the grafting structure of P(VDF-CTFE)-*g*-PMMA synthesized from $FeCl_2/PPh_3$ and CuCl/BPy catalyzed ATRP process and corelating the experimental results to kinetics analysis, the influence of less active initiator on the living performance of ATRP and the evolution of growing polymer chains was clearly disclosed.

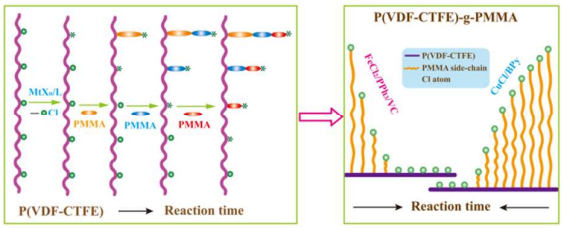

Influence of Less Active Initiator on the Living Performance of Atom Transfer Radical Polymerization and the Structure of Grafted Copolymer Synthesized

Honghong Gong,[a] Junjie Li,[a] Daming Di,[b] Na Li[b] and Zhicheng Zhang*[a]

[a] *Department of Applied Chemistry, MOE Key Laboratory for Nonequilibrium Synthesis and Modulation of Condensed Matter, School of Science, Xi'an Jiaotong University, Xi'an, P. R. China,710049, Tel.:* +86 29 82663937; fax: +86 29 82668559; *E-mail: zhichengzhang@mail.xjtu.edu.cn*

[b] *Department of Chemical Engineering, School of Chemical Engineering and Technology, Xi'an Jiaotong University, Xi'an 710049 Shaanxi, P. R. China. 710049*

Graphical Abstract

By monitoring the grafting structure of P(VDF-CTFE)-*g*-PMMA synthesized from $FeCl_2/PPh_3$ and CuCl/BPy catalyzed ATRP process and corelating the experimental results to kinetics analysis, the influence of less active initiator on the living performance of ATRP and the evolution of growing polymer chains was clearly disclosed.

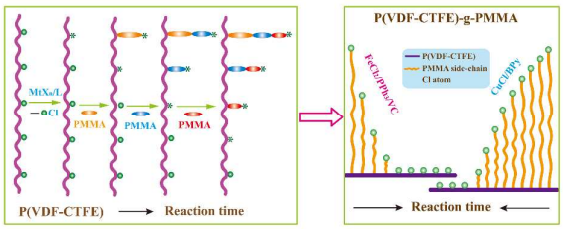

Influence of Less Active Initiator on the Living Performance of Atom Transfer Radical Polymerization and the Structure of Grafted Copolymer Synthesized

Honghong Gong,[a] Junjie Li,[a] Daming Di,[b] Na Li[b] and Zhicheng Zhang*[a]

[a] *Department of Applied Chemistry, MOE Key Laboratory for Nonequilibrium Synthesis and Modulation of Condensed Matter, School of Science, Xi'an Jiaotong University, Xi'an, P. R. China,710049*

[b] *Department of Chemical Engineering, School of Chemical Engineering and Technology, Xi'an Jiaotong University, Xi'an 710049 Shaanxi, P. R. China. 710049*

Correspondence: Tel.: +86 29 82663937; fax: +86 29 82668559

E-mail: *zhichengzhang@mail.xjtu.edu.cn*

Abstract

In an effort to precisely describe the structure of polymers synthesized *via* ATRP initiated with less active initiator and clearly understand the evolution of the polymer chains, methyl methacrylate (MMA) was grafted onto poly(vinylidene fluoride-chlorotrifluoroethylene) (P(VDF-CTFE)) catalyzed with two different catalysts. The detailed structure information of the grafted copolymers, including the grafting density, the average side chain length, the average molecular weight and its distribution, has been carefully determined by removing the homopolymers from the resultant copolymer and converting the uninitiated Cl atom into H atom, which has been finely correlated to the reaction conditions. By correlating the structure information to kinetics analysis, the evolution of the side chains has been clearly demonstrated step-by-step. The low initiation activity of C-Cl and the low redox capability of catalyst system are responsible for the wide distribution, the low grafting density and the slow growing polymer chains. The results may help to understand not only the polymer structure synthesized from ATRP process more precisely but also the evolution of the polymer chains under different reaction conditions more directly.

1 Introduction

With the continuous increasing request of desired polymer materials, design, precise synthesis and characterization, and processing of well-defined polymers with specific properties for targeted applications are becoming the future developing trend of polymer science and engineering. Before 1980s, polymers with high molecular weight uniformity and precisely designed structure could only be prepared *via* living ionic polymerization, a process that requires very stringent experimental conditions or the other complicated strategies in multi steps.[1] Living/controlled radical polymerization (CRP) emerged in 1990s and was developed quickly as one of the most robust and powerful techniques for polymer synthesis during the past thirty years.[2] It combines the desirable attributes of conventional free radical polymerization (e.g., the ability to polymerize a wide range of monomers, tolerance of various functionalities in monomer and solvent and inexpensive reaction conditions) and the advantages of living ionic polymerization techniques (e.g., preparation of polymer with low molecular weight distribution (M_w/M_n) and chain-end functionalized polymers).[3] Atom transfer radical polymerization (ATRP), as one of the most representative examples among all the CRP methods discovered by both Matyjaszewski[4] and Sawamoto[5] in 1995 adapted from the concept of continuous atom transfer radical addition (ATRA), has been developed as one of the most powerful and robust tools for preparing new polymeric materials with controlled molecular weights and well-defined architectures during past decades.[6-12] Especially, it provides a desirable strategy to synthesize polymers with different topology structures such as

the star-like, dendritic, hyperbranched, multi-blocked and comb-like grafted polymers.[13-25]

The control/living characteristics in ATRP are established through a dynamic, quick, and reversible equilibrium between dormant and active polymerization states, which promote concurrent growth of each polymer chain and mediate the concentration of propagating radicals (P_n^*) (Scheme 1). The molecular weight improving against reaction time and polydispersity index (PDI) of homopolymers synthesized from ATRP could be easily determined from Gel Permeation Chromatography (GPC), which are essential parameters for evaluating the living or controlling characteristic of the polymerization. The ATRP equilibrium constant (K_{ATRP}), defined as the ratio of activation (k_{act}) to deactivation (k_{deact}) rate constants, is dependent on a variety of reaction parameters and especially strongly influenced by the structure and properties of involved chemical components including the alkyl halide (R-X, initiator; P_n-X, polymer), catalysts (Mt^n/L, Mt = Cu, Ru, Fe, etc.) and monomers, each capable of altering K_{ATRP} over 6 orders of magnitude.[26] Usually, the initiators with the similar structure of monomer (R-X and P_n-X are treated as the same species) or low C-X bonding energy and catalysts with high activity were employed in ATRP to ensure the consistent polymerization rate (R_p) of all the active sites,[27] which is essential to prepare polymers with narrow molecular weight distribution and well-defined architecture. If the activity of initiator R-X is too low, poorly controlled polymerization together with the wide molecular weight distribution in the resultant copolymer would be observed. However, the information including how many

initiators are involved in the polymerization and how many polymer chains are thermally initiated could not be obtained in ATRP process initiated with small molecular initiators.

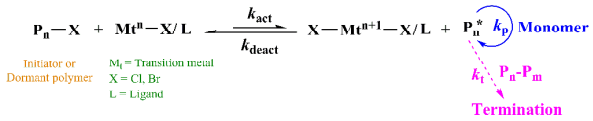

Scheme 1 Traditional ATRP mechanism.

Meanwhile, the structure of the initiator is not always as selectable as catalysts when ATRP is used in polymer modification to prepare blocked or grafted copolymers, where the pristine polymer with certain structure is reserved as initiators. In these cases, the structure and activity difference between the initiating (R-X) and propagating (RM_n-X) species is responsible for the poorly controlled polymerization. Especially, it would lead to the unpredictable structure of the resultant grafted or blocked copolymers synthesized in ATRP process. Different from synthesizing homopolymers in this process, the influence of thermally initiated homopolymerization of monomers on the structure characterization of the resultant grafted or blocked copolymers has to be concerned and excluded completely. However, the absence of characterization methods makes the detailed structure information of the resultant copolymers, such as the length and distribution of the growing chains, the grafting densities and how the side chains growing step-by-step, could hardly be obtained, although they exhibit vital influence on the properties of the copolymers. That is also why the investigation on the precise structure of the grafted copolymers and the living characteristics of ATRP in these cases has been rarely

mentioned.

Poly(vinylidene fluoride) (PVDF)-based fluoropolymers are very interesting niche specialty polymeric materials for their outstanding properties.[28,29] To extend the application area of fluoropolymers, many chemical methods were developed to modify commercial fluoropolymers by introducing functional groups onto them during past decades.[30-34] Poly(vinylidene fluoride-chlorotrifluoroethylene) (P(VDF-CTFE)), as one of the most utilized commercial fluoropolymers (mostly as elastomers), comprises CTFE units with pendant secondary halogen atoms, which might serve as potential ATRP initiators. M. F. Zhang et al.[35] firstly reported the grafting copolymerization of styrene (St) and *i*-Butyl methacrylate (BMA) onto P(VDF-CTFE) *via* ATRP process in 2005. After that, many research groups employed the strategy to modify commercial fluoropolymers in order to obtain various products with different performance and applications.[36-41] E. M. W. Tsang and his coworkers[42] reported two kinds of proton-conducting membranes of P(VDF-CTFE)-*g*-SPS (SPS, sulfonated polystyrene) and P(VDF-HFP)-*b*-SPS (HFP, hexafluoropropylene) possessed similar composition but considerably different architecture. The structure of the copolymer showed significant effect on the morphology of the membranes and, in turn, their ion conducting and water swelling properties. Z. C. Zhang et al[43] also studied the property of two similar polymers membrane of P(VDF-CTFE)-*g*-SPS with different grafting densities but consistent compositions. The grafting densities showed great influence on the congregation of the hydrophilic phases in the membrane and the water uptaking properties. More recently, our group synthesized

P(VDF-CTFE)-*g*-PEMA (PEMA, poly(ethyl methacrylate)) through activators regenerated by electron transfer for ATRP (ARGET-ATRP) route using CuCl/BPy (BPy, 2, 2'-Bipyridine) as catalyst and investigated its high-field antiferroelectric behavior for the energy storage application.[44,45] Although the average side length and the grafting densities could be varied and estimated in previous work, more detailed structure information of the grafted copolymers and how the grafting chains grows during the polymerization process have rarely been presented. Based on the previous investigation, C-Cl bonds on P(VDF-CTFE) is less active than its propagation species RM_n-Cl, which is expected to result in wide distribution of the side chain length and poor controlled characteristics in ATRP polymerization. Whereas, simple parameters provided in previous investigation could neither help to describe the structure of the copolymer precisely nor understand the process of the polymerization clearly.

In an effort to describe the structure of copolymer formed precisely and illustrate how the polymer chains were growing in ATRP process initiated with less active initiator, such as CTFE on P(VDF-CTFE) in the present work, ATRP of methyl methacrylate (MMA) catalyzed with two types of catalyst system with different catalyst activity such as $FeCl_2/PPh_3$ and CuCl/BPy were conducted, respectively. To eliminate the influence of homopolymerization on the structure characterization of resultant copolymer and ATRP process, the thermally initiated PMMA homopolymers were completely removed by chloroform ($CHCl_3$) by dint for the different solubility of grafted copolymer and homo-PMMA in $CHCl_3$. By converting all the C-Cls on P(VDF-CTFE)-*g*-PMMAs into C-Hs catalyzed with tributyltin/azobisisobutyronitrile

(nBu$_3$SnH/AIBN) and analyzing the composition obtained from proton nuclear magnetic resonance (^{1}H NMR) results, the precise molar content of C-Cl sites onto P(VDF-CTFE) initiated could be determined, which is the key for characterizing the real structure of the grafted copolymer. By analyzing the copolymers obtained at different time intervals, the detailed structure information and the evolution of side chains have been determined. How the activity of R-Cl initiator influences the initiation and propagation processes of ATRP were clearly illustrated by correlating the structure information to the kinetic results obtained.

2 Experimental

2.1 Materials

P(VDF-CTFE) (31508) with 9 mol% CTFE was purchased from Solvay Solexis. $FeCl_2$ (Shanghai Chemical Reagents Co., 98%) was washed with acetone and dried under vacuum at 60^{o}C before use. Triphenylphosphine (PPh_3) was obtained from Henwns Biochem Technologies LLC (Tianjin, China) and used as received. Methyl methacrylate (MMA) was washed twice with 5 wt% NaOH aqueous solution and twice with water, dried overnight with $MgSO_4$, distilled under reduced pressure, and stored under N_2 at -20^{o}C. nBu$_3$SnH and AIBN were obtained from Aladdin Reagent Co. and used as received. Dimethyl sulfoxide (DMSO) and tetrahydrofuran (THF) were commercial available and distilled under reduced pressure from CaH_2 before used. All the other chemicals were commercially available and used as received.

2.2 Grafting PMMA onto P(VDF-CTFE) *via* ATRP process

A typical synthesis procedure of P(VDF-CTFE)-*g*-PMMA grafted copolymers is

following the procedure reported in literature.[35] Into a N_2 purged 250 mL three-necked glass bottle, 2 g of P(VDF-CTFE) (VDF/CTFE = 91/9 mol%) (containing 2.6 mmol Cl atom), 60 mL of DMSO, 2.6 mmol of $FeCl_2$, 5.2 mmol of PPh_3 and a given amount of reducing agent were introduced and heated at required temperature in N_2 atmosphere with vigorous stirring. Samples were taken at regular time intervals followed by precipitating in H_2O/CH_3OH (1 : 1 in volume) mixture, washing five times with methanol and drying for 8 h at 40°C under reduced pressure. A general procedure for the synthesis of P(VDF-CTFE)-*g*-PMMA was shown in Scheme 2. ^{1}H NMR was applied to calculate the overall MMA conversion including both the MMA grafted onto P(VDF-CTFE) and PMMA homopolymer. The resultant polymer was soaked with chloroform for three times to remove PMMA homopolymer and the composition of P(VDF-CTFE)-*g*-PMMA could be obtained from the ^{1}H NMR results as discussed later.

2.3 *n*Bu$_3$SnH/AIBN hydrogenation process of P(VDF-CTFE)-*g*-PMMA

As suggested in Scheme 2, the hydrogenation of P(VDF-CTFE)-*g*-PMMA was conducted to determine the content of CTFE uninitiated in the resultant copolymer following the procedure reported in the literature.[46-48] In a 100 mL three-necked flask with magnetic stirring bar, 1.0 g of P(VDF-CTFE)-*g*-PMMA and 0.086 g (0.52 mmol) of AIBN were added and degassed three times with dry nitrogen-vacuum cycles. 40 mL of dried THF was purged with dry nitrogen for about 30 min and transferred into the flask by a nitrogen-protected syringe. 0.56 mL (2.08 mmol) of *n*Bu$_3$SnH was injected into the solution using a syringe as soon as the polymer was well dissolved

under vigorous stirring. The hydrogenation reaction was carried out in an oil-bath at 60°C for 24 h. The resultant was obtained by precipitating the reaction mixture into *n*-hexane and purified by extracting the precipitant with hot *n*-hexane in a Soxhlet extractor for 24 h followed by dried at 60°C under reduced pressure for 8 h. The chemical composition of the resultant copolymer was determined with ^{1}H NMR.

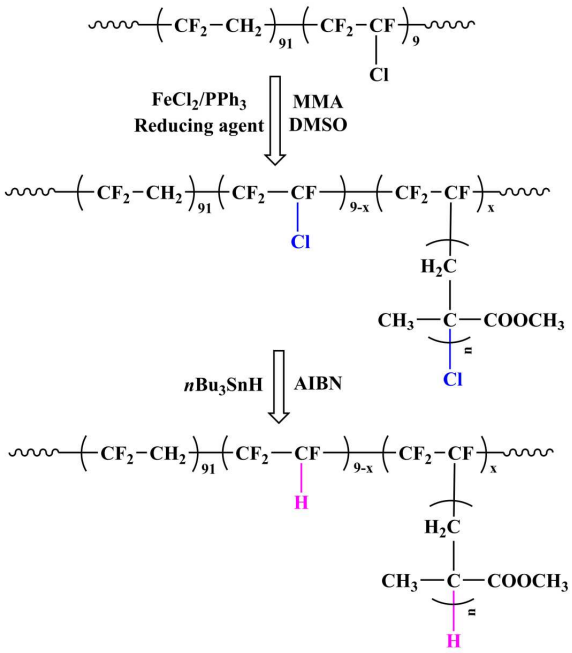

Scheme 2 Schematic illustration of the synthesis and hydrogenation process of P(VDF-CTFE)-*g*-PMMA copolymer.

2.4 Instrumentation and characterization

^{1}H NMR spectra was obtained using a Bruker (Advance III) 400 MHz spectrometer with acetone-d_6 as solvent and tetramethylsilane as an internal standard. Fourier transform infrared (FTIR) spectroscopy of the films was recorded on a Tensor 27 (Bruker, Germany) with a resolution of 1-0.4 cm^{-1}. Differential scanning calorimetric (DSC) analysis was conducted on a Netzsch DSC 200 PC (Netzsch, Germany) in a

nitrogen atmosphere at a scanning rate of $10^{o}C/min^{-1}$ after a circle of quick heating ($20^{o}C/min^{-1}$) and cooling ($20^{o}C/min^{-1}$) to remove the thermal history.

3 Results and discussion

3.1 Characterization of P(VDF-CTFE)-*g*-PMMA Copolymer

The grafting of MMA onto P(VDF-CTFE) could be identified on FTIR spectroscopy as shown in Fig. 1S. The result clearly confirms the presence of PMMA segments. Thermal property of P(VDF-CTFE)-*g*-PMMA was characterized with DSC analysis as shown in Fig. 2S.

The structure of P(VDF-CTFE)-*g*-PMMA was confirmed with ^{1}H NMR as shown in Fig. 1. Two peaks at 2.2–2.7 ppm (I_1) and 2.7–3.2 ppm (I_2) in the original P(VDF-CTFE) could be attributed to the protons on VDF units in head-head (–CF_2–C***H***$_2$–C***H***$_2$–CF_2–) and head-tail (–CF_2–C***H***$_2$–CF_2–C***H***$_2$–) connection, respectively. The shoulder peak at 3.2–3.6 ppm (I_3) adjacent to the main peak at 2.7–3.2 ppm could be assigned to the proton on VDF connected with CTFE in head-tail connection (–CF_2–C***H***$_2$–CFCl–CF_2–). Comparing with the ^{1}H NMR spectrum of P(VDF-CTFE), new signals emerging at 3.6–3.8 ppm (I_4) were assigned to the protons on –OC***H***$_3$ of MMA. Meanwhile, the proton signals on VDF adjacent to CTFE were decreasing at 3.2–3.6 ppm as more MMA units were grafted. Overall MMA conversion (%) and MMA grafted onto P(VDF-CTFE) (%) were calculated from ^{1}H NMR of the resultant copolymer before and after removing homo-PMMA by soaking with $CHCl_3$ following eq (1) and eq (2),

$$\text{MMA} \quad Conversion\,(\%) = \frac{2}{3} \times \frac{I'_4}{I'_1 + I'_2 + I'_3} \times \frac{[VDF]_0}{[MMA]_0} \times 100\% \qquad \text{eq (1)}$$

$$\text{MMA}\quad grafted\,(\%) = \frac{2}{3} \times \frac{I_4}{I_1 + I_2 + I_3} \times \frac{[VDF]_0}{[MMA]_0} \times 100\% \qquad \text{eq (2)}$$

where I'_1-I'_4 and I_1-I_4 are referring to the integral of peaks as assigned above on ^{1}H NMR of resultant polymer before and after PMMA removed, $[VDF]_0$ and $[MMA]_0$ are the initial concentration of VDF units and monomer. The composition of the P(VDF-CTFE)-*g*-PMMA referring to the molar ratios of VDF, CTFE and MMA units was estimated from eq (3) based on the assumption that VDF units were not involved in the polymerization.

$$\text{VDF/CTFE/MMA} = 91 : 9 : (\frac{2}{3} \times \frac{I_4}{I_1 + I_2 + I_3} \times 91) \qquad \text{eq (3)}$$

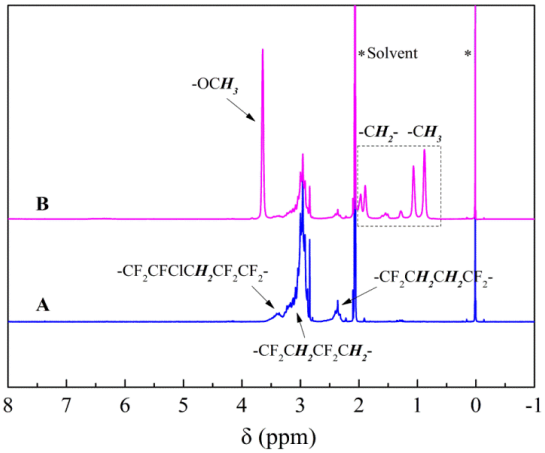

Fig. 1 ^{1}H NMR spectra of (A) Pristine P(VDF-CTFE) and (B) P(VDF-CTFE)-*g*-PMMA.

3.2 Synthesis of P(VDF-CTFE)-*g*-PMMA catalyzed with $FeCl_2/PPh_3$

In an effort to investigate the influence of initiator activity on the structure of the grafted copolymers, the initiation and propagation reaction rates, $FeCl_2/PPh_3$ and CuCl/BPy catalysts were employed to catalyze the grafting polymerization of PMMA onto P(VDF-CTFE). Comparing to CuCl/BPy catalyst system, $FeCl_2/PPh_3$ exhibits

lower K_{ATRP} and is designed to synthesize P(VDF-CTFE)-*g*-PMMA with different structure. The composition of P(VDF-CTFE)-*g*-PMMAs synthesized from $FeCl_2/PPh_3$ under varied conditions was listed in Table 1S. To avoid the elimination reaction of P(VDF-CTFE) catalyzed by *N*-containing compounds, DMSO was utilized as solvents in all the polymerization. As shown in Table 1S, very low conversion of MMA was obtained in all the resultant copolymers. Prolonging the reaction time, conducting the polymerization at elevated temperature and increasing the catalysts concentration do not show significant effect on increasing the polymerization of MMA. Following the previous reports, that might be attributed to the low k_{act}/k_{deact} (or K_{ATRP}) of P(VDF-CTFE) catalyzed with $FeCl_2/PPh_3$, which means either the life or the concentration of the free radicals generated is too small for the propagation reaction to take place. In order to drive the equilibrium in Scheme 1 to the right direction, prolong the life time of free radicals and increase the conversion of MMA, zero-valent metallic, inorganic sulfites and small organic molecules were employed as reducing agent (RA). The detailed experimental results were shown in Table 2S, and the results indicated that VC as reducing agent showed the highest MMA conversion and very low content of homo-PMMA. That means VC is the most desirable reducing agent for the ATRP of MMA initiated with P(VDF-CTFE), which is used in all the following copolymerization in $FeCl_2/PPh_3$ systems.

3.3 Structure of P(VDF-CTFE)-*g*-PMMA catalyzed with $FeCl_2/PPh_3$ System

Usually, the structure information of the grafted copolymers could hardly be obtained more than the average side length and the overall units grafted as discussed

above. The conversion of the monomer could be determined by measuring the weight of copolymer obtained. The overall monomers grafted onto the pristine polymer could be obtained by subtracting the homopolymerized monomers from the overall converted ones. The average grafted side chain length (number of the grafted units) could be calculated by dividing the molar content of grafted monomers with the molar content of overall active sites based on the assumption that all the C-X active sites were involved. These parameters are sufficient and precise to describe the structure of comb-like grafted copolymers with consistent length of side chains. However, if the activity of the pristine polymer as macro initiator is not sufficient high, some of the C-X active sites may not be initiated. Assuming all of them are initiated as reported in literature[40] would lead to misleading structure information including overestimated grafting density, underestimated grafting length as well as varied length distribution of the grafting side chains. Unfortunately, the absence of characterization method makes it impossible to determine how many active sites are getting involved in polymerization and how many polymer chains are thermally initiated in most cases.

In present work, C-Cl of CTFE units on P(VDF-CTFE) is designed as active sites and expected to form macro free radicals followed by the initiation and propagation reactions. However, the low activity of C-Cl in this structure could not ensure all the C-Cl to be activated based on previous results. Then the amount of C-Cl bonds getting involved in the polymerization has to be determined to obtain the precise structure information of the grafted copolymer. Fortunately, the uninitiated CTFE content could be detected with ^{1}H NMR by converting Cl atoms into H atoms *via* a hydrogenation

process catalyzed with nBu$_3$SnH/AIBN as suggested in Scheme 2. For comparison purpose, both P(VDF-CTFE) and P(VDF-CTFE)-*g*-PMMA were fully hydrogenated and ^{1}H NMR spectra of P(VDF-CTFE) and P(VDF-CTFE)-*g*-PMMA together with their full hydrogenated products P(VDF-TrFE) and P(VDF-TrFE)-*g*-PMMA were presented in Fig. 2. The shoulder peak at 3.2–3.6 ppm in P(VDF-CTFE) and P(VDF-CTFE)-*g*-PMMA (Fig. 2A and Fig. 2C) was assigned to the proton on VDF connected with CTFE in head-tail connection (–CF_2–C***H***$_2$–CFCl–CF_2–), which is completely disappeared in the full hydrogenation product P(VDF-TrFE) and P(VDF-TrFE)-*g*-PMMA (Fig. 2B and Fig. 2D). Meanwhile, new signals emerging at 5.3–5.8 ppm (I_5) were assigned to the protons on TrFE (–CF_2C***H***–) converted from unreacted CTFE in P(VDF-CTFE)-*g*-PMMA. Therefore, the molar concentration of un-initiated CTFE units could be calculated from the following equation,

$$[\mathrm{CTFE}]_t = \frac{2 \times \mathrm{I}_5}{\mathrm{I}_1 + \mathrm{I}_2} \times [\mathrm{VDF}]_0 \qquad \text{eq (4)}$$

Accordingly, the molar percentage of CTFE initiated (CTFE initiated%) could be calculated by subtracting the molar percentage of unreacted CTFE from all the overall CTFE units input with the following eq (5),

$$\text{CTFE initiated\%} = \frac{[\mathrm{CTFE}]_0 - [\mathrm{CTFE}]_t}{[\mathrm{CTFE}]_0} \times 100\% \qquad \text{eq (5)}$$

where $[\mathrm{CTFE}]_0$ and $[\mathrm{CTFE}]_t$ are the molar concentration of overall CTFE units input and unreacted CTFE remained in the grafted copolymers as discussed above. The real grafting densities (D_{PMMA}) on 100 main chain units and average polymerization degree (DP) of the grafted copolymers could be obtained by the following equations,

$$D_{PMMA} = 9\% - \frac{2 \times I_5}{I_1 + I_2} \times 91\% \qquad \text{eq (6)}$$

$$DP = \frac{Conversion \times [MMA]_0}{[CTFE]_0 - [CTFE]_t} \qquad \text{eq (7)}$$

Taking the sample of entry 9 in Table 2S as an instance, the D_{PMMA} is obtained as 1.1 branches in every 100 main chain units, which means only 12% of overall CTFE units input was initiated. Therefore, the real DP calculated from eq (7) is 39.0, which is much bigger than that (4.7) calculated from the overall MMA grafted divided by overall CTFE input ($[CTFE]_0$) directly. Apparently, most of the CTFE units have not been initiated as concerned although MMA conversion has been over 16%.

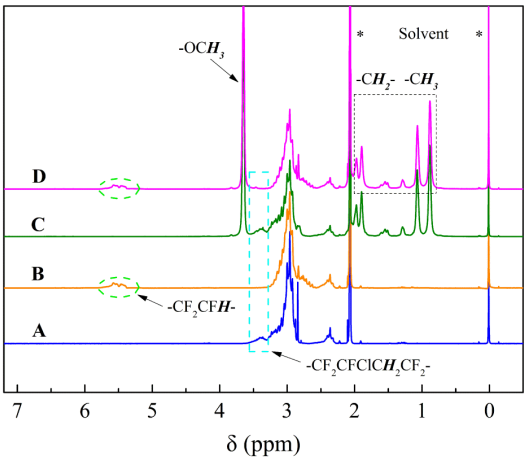

Fig. 2 ^{1}H NMR spectra of (A) P(VDF-CTFE), (B) P(VDF-TrFE), (C) P(VDF-CTFE)-*g*-PMMA and (D) P(VDF-TrFE)-*g*-PMMA.

To illustrate the initiation and propagation process more clearly, the grafting polymerization was conducted in 1 h and samples were taken at an interval of 10 min. The percentage of CTFE initiated and MMA grafted in all the copolymers as a function of the reaction time were shown in Fig. 3. As reaction time increases, CTFE

initiated is increasing slowly and linearly, which means the molar concentration of active species RM_n-Cl (n = 1, 2, 3…) formed is increasing in linear against reaction time with a very small slope (about 0.13%/min). The percentage of grafted MMA is increasing in linear as well as reaction time increases. In an ideal living (or controlled) radical polymerization system, all the active sites are supposed to be initiated immediately and the amount of the active sites should be a constant during the propagation process since the chain termination reaction is negligible. As a result, all the active sites have the same possibility and reaction rate to insert monomers during the propagation process characterized with a very small distribution of resultant polymer and linearly increased monomer conversion against reaction time. Apparently, the grafted copolymer synthesized in present work is far from the ideal case. First of all, R-Cl is converting to RM-Cl slowly as reaction time increases. However, the following propagation of RM-Cl is much faster comparing to the initiation of R-Cl. As a result, the polymer chain formed from RM-Cl is increasing quickly until next R-Cl is activated and converted into RM-Cl. As more RM-Cl and RM_n-Cl formed, the increasing speed of polymer chain length is reduced since the MMA conversion is increasing in linear, which means the earlier of the grafting polymer chain formed, the longer chain length would be observed. Meanwhile, a large quantity of CTFE units is not initiated since the initiation reaction is rather slow. Therefore, the structure of the grafted copolymer could be illustrated as a grafted copolymer containing a small quantity of side chains and the chain length is varied in a large scale as shown in Scheme 3.

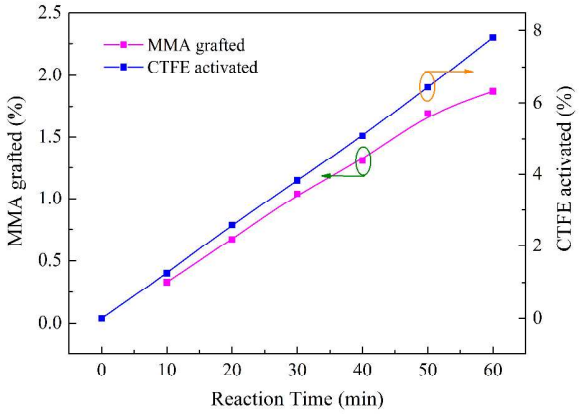

Fig. 3 MMA grafted (%) and CTFE activated (%) in the P(VDF-CTFE)-*g*-PMMA calculated from eq (2) and eq (5) catalyzed with $FeCl_2/PPh_3$/VC.

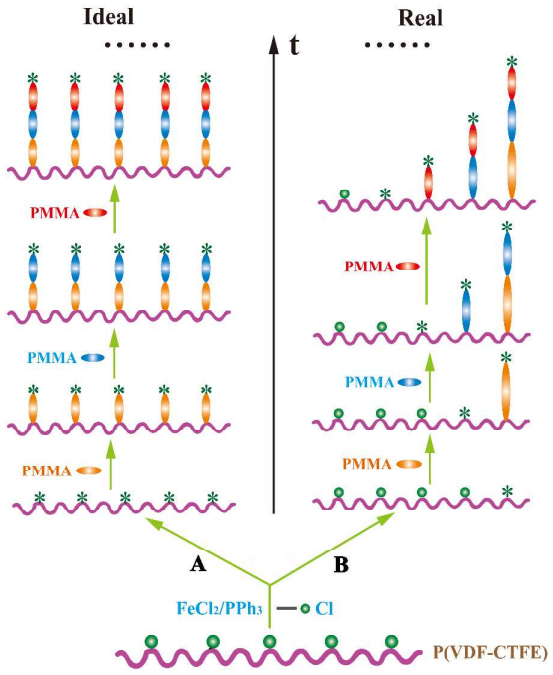

Scheme 3 Structure evolution of grafted copolymers synthesized from ATRP process. (A, Ideal case; B, Real case).

3.4 Effect of catalyst system on the structure of P(VDF-CTFE)-*g*-PMMA

From the above discussion, it is not difficult to find out that the formation of the structure is mainly due to the reactivity difference of initial initiator (R-Cl) and the propagation species (RM_n-Cl) with $FeCl_2/PPh_3$ catalyst. Besides the chemical bonding

difference of R-Cl and RM_n-Cl, catalyst system should influence the reactivity as well which has been well reported in ATRP system.[26] Therefore, it is logical to believe that the different catalyst system should affect the structure of grafted copolymer as well. For the comparison purpose, CuCl/BPy was used as catalyst for the synthesis of P(VDF-CTFE)-*g*-PMMA under the consistent reaction conditions. Samples were taken at a time interval of 10 min, and all the copolymers were extracted to remove homopolymers followed by hydrogenated with nBu$_3$SnH/AIBN as well for the structure characterization. The MMA grafted (%) and the percentage of CTFE units activated in all the samples were calculated through eq (2) and (5) and summarized in Table 1. As reaction time increases, both the molar percentage of CTFE activated and MMA grafted onto P(VDF-CTFE) catalyzed with CuCl/BPy are increasing and exhibit the similar trend as that of $FeCl_2/PPh_3$/VC. However, much higher CTFE content and MMA monomer have been consumed in CuCl/BPy system, which could be attributed to the much higher activity of CuCl/BPy catalyst than that of $FeCl_2/PPh_3$/VC. That also suggests the grafted copolymers should possess rather different structure based on the activated CTFE content and MMA grafted onto P(VDF-CTFE).

Table 1 MMA grafted (%) and CTFE initiated (%) in P(VDF-CTFE)-*g*-PMMA catalyzed with two kinds of catalyst determined by ^{1}H NMR.

Polymer structure	Reaction time (min) t_i (i = 1, 2, …, 6)					
	t_1=10min	t_2=20min	t_3=30min	t_4=40min	t_5=50min	t_6=60min

$FeCl_2/PPh_3/VC$ Catalyst[a]	MMA grafted (%)	0.33	0.67	1.03	1.40	1.79	2.05
	CTFE initiated (%)[c]	1.25	2.58	3.83	5.08	6.44	7.80
CuCl/BPy Catalyst[b]	MMA grafted (%)	0.93	4.40	10.26	17.09	22.43	25.56
	CTFE initiated (%)[c]	13.73	23.92	31.56	37.61	41.68	43.63

[a] Experimental conditions: [R-Cl]/[$FeCl_2$]/[PPh_3]/[VC]/[MMA] = 1 : 1 : 2 : 1 : 80 in molar, T = 100°C, 5 g P(VDF-CTFE) as initiator and 150 mL DMSO as solvent.

[b] Experimental conditions: [R-Cl]/[CuCl]/[BPy]/[MMA] = 1 : 1 : 2 : 80, in molar, T = 100°C, 5 g P(VDF-CTFE) as initiator and 150 mL DMSO as solvent.

[c] The molar percentage of CTFE initiated is calculated from eq (5).

To obtain the more detailed structure information of the grafted copolymers and illustrate how the grafted copolymers were formed and propagated, the molar content of active sites (RM-Cl) formed in different time intervals was calculated from eq (8),

$$n_i = [(\text{CTFE initiated}\%)_{t_i} - (\text{CTFE initiated}\%)_{t_{i-1}}] \times [\text{CTFE}]_0 \ mmol \qquad \text{eq (8)}$$

where t_i (i = 1, 2, …, 6) is referring to the different reaction time. t_1 means the polymerization in first 10 mins, t_2 represents the polymerization in 20 mins, and so on. As shown in Table 2, a consistent molar content of CTFE (0.008-0.009 mmol/min) was initiated and formed RM-Cl in every time intervals in $FeCl_2/PPh_3$/VC system, which means the concentration of overall RM_n-Cl (n = 1, 2, 3…) species are increasing linearly against reaction time as shown in Fig. 4. Differently, the CTFE

molar content activated by CuCl/BPy in different time intervals is decreasing rapidly from (0.072 mmol/min to 0.01 mmol/min) as reaction time increases. That means many CTFE units are quickly initiated and converted into RM-Cl followed by chain propagation process. The initiation speed of CTFE is quickly reduced and the concentration of overall RM_n-Cl (n = 1, 2, 3…) species is improving but deviating linear relationship against reaction time as shown in Fig. 4.

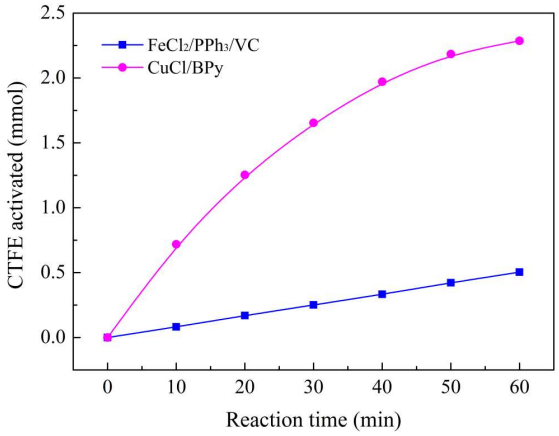

Fig. 4 Molar number of initiated CTFE versus reaction time during ATRP process catalyzed with $FeCl_2/PPh_3$/VC and CuCl/BPy.

The grafting propagation process was characterized with the average polymerization degree ($\overline{DP}_i$ i = 1, 2, …, 6) of PMMA grafted on P(VDF-CTFE) in different time intervals. $\overline{DP}_i$ could be calculated by dividing the molar content of grafted MMA in the time interval of i with molar content of overall RM_n-Cl (n = 1, 2, 3…) formed in time t from the following eq (9),

$$\overline{DP}_i = \frac{(\text{MMA grafted (\%)}_{t_i} - \text{MMA grafted (\%)}_{t_{i-1}}) \times [\text{MMA}]_0}{(\text{CTFE initiated (\%)}_{t_i}) \times [\text{CTFE}]_0} \quad \text{eq (9)}$$

where MMA grafted (%) and CTFE initiated (%) in different time intervals are from Table 1. $\overline{DP}_i$ of the MMA grafted with $FeCl_2/PPh_3$/VC catalyst is dropping quickly

as reaction time increases as shown in Table 2. That means the average growing speed of each grafting chains is decreasing as a function of reaction time. Unlike $FeCl_2/PPh_3$/VC catalyst, $\overline{DP_i}$ of the MMA grafted with CuCl/BPy catalyst increases firstly and maintains a constant for a while before it starts to drop. That may be attributed to the enhanced concentration of RM_n-Cl (n = 1, 2, 3…) species and the decreased MMA concentration. The results strongly indicate that the reaction reactivity of CuCl/BPy catalyst is higher than that of $FeCl_2/PPh_3$/VC.

Table 2 $\overline{DP_i}$, n_i (mmol), molar percentage (x_{n_i}), weight percentage (w_{n_i}) and molecular weight M_{n_i} (g/mol) of grafted PMMA onto P(VDF-CTFE) in different time intervals determined by ^{1}H NMR.

Time interval (min)[a]		i = 1 (0-10)	i = 2 (10-20)	i = 3 (20-30)	i = 4 (30-40)	i = 5 (40-50)	i = 6 (50-60)
$FeCl_2/PPh_3$/VC Catalyst	n_i (*mmol*)[b]	0.082	0.087	0.082	0.082	0.089	0.089
	$\overline{DP_i}$[c]	21.0	10.5	7.6	5.8	4.8	2.7
	M_{n_i}[d]	5,250	3,140	2,090	1,330	750	270
	x_{n_i} (%)[e]	16.03	17.05	16.05	16.05	17.42	17.42
	w_{n_i} (%)[f]	39.63	25.47	15.96	10.16	6.21	2.24
CuCl/BPy Catalyst	n_i (*mmol*)	0.719	0.534	0.401	0.317	0.213	0.102
	$\overline{DP_i}$	5.4	11.6	14.9	14.5	10.3	5.7
	M_{n_i}	6,240	5,700	4,540	3,050	1,600	570
	x_{n_i} (%)	31.45	23.36	17.54	13.87	9.32	4.46
	w_{n_i} (%)	41.87	28.40	16.99	9.02	3.18	0.54

[a] The time interval between two adjacent time point. For example: (10-20) is referring to the second interval of the reaction namely the polymerization conducted between the 10th and 20th minute since the reaction starts.

[b] The molar content of CTFE initiated in different intervals is calculated from eq (8).

[c] The average polymerization degree of grafted PMMA on all initiated CTFEs is calculated from eq (9).

[d] The average molecular weight of PMMA side chains formed in different time intervals is obtained from eq (10).

[e, f] The molar and weight percentage of side chains formed in different time intervals are calculated from eq (11) and eq (12), respectively.

In addition, the average molecular weight of every PMMA side chains formed in different time intervals (M_{n_i}, i = 1, 2, …, 6) could be obtained by accumulating all the amount of MMA units grafted during the polymerization processes since CTFEs were initiated (as suggested in eq (10)),

$$M_{n_i} = \sum_{j=i}^{6} \overline{DP}_i \times M_0 \qquad (i = 1, 2, \ldots, 6) \qquad \text{eq (10)}$$

where M_0 is the molecular weight of monomer. As listed in Table 2, the molecular weight of the grafting polymer chains formed in different time intervals catalyzed with both catalysts shows the similar decreasing trend as reaction time increases. That means the earlier the grafted chains are generated, the longer grafted chain length would be obtained as suggested in Scheme 3. The difference is the molecular weight of side chains obtained from $FeCl_2/PPh_3$/VC system is reducing more quickly than

that of CuCl/BPy. That means the length difference of side chains obtained from $FeCl_2/PPh_3$/VC system is more significant than that of CuCl/BPy.

Meanwhile, the molar (x_i) and weight (w_i) percentage of side chains formed in different time intervals with molecular weight of M_{n_i} could be obtained from the following equations,

$$x_i = n_i \Big/ \sum_{i=1}^{6} n_i \qquad (i = 1, 2, \ldots, 6) \qquad \text{eq (11)}$$

$$w_i = M_{n_i} \times n_i \Big/ (\text{MMA grafted (\%)})_{t_6} \times [\text{MMA}]_0 \times \text{M}_0 \qquad (i = 1, 2, \ldots, 6) \qquad \text{eq (12)}$$

Apparently, the molar percentage of different molecular weight of side chains has a similar value when $FeCl_2/PPh_3$/VC is used as catalyst as listed in Table 2. Differently, the molar percentage distribution of PMMA side chains is relatively concentrated when CuCl/BPy is used as catalyst.

To illustrate the side chain length difference of copolymers obtained from two catalysts more clearly, the number-average molecular weight ($\overline{M}_n$) and weight-average molecular weight ($\overline{M}_w$) of the PMMA grafted in 1 h as well as the PDI are estimated from the following equations (eq 13, 14 and 15) according to the results listed in Table 3.

$$\overline{M}_n = \sum_{i=1}^{6} x_i M_{n_i} \qquad \text{eq (13)}$$

$$\overline{M}_w = \sum_{i=1}^{6} w_i M_{n_i} \qquad \text{eq (14)}$$

$$\text{PDI} = \frac{\overline{M}_w}{\overline{M}_n} \qquad \text{eq (15)}$$

As shown in Table 3, the average molecular weight of PMMA grafted onto

P(VDF-CTFE) catalyzed with CuCl/BPy is larger than that of $FeCl_2/PPh_3/VC$, which confirms their catalytic activity difference as discussed above. Meanwhile, the smaller PDI obtained from CuCl/BPy may address the better controllability of CuCl/BPy catalyst than $FeCl_2/PPh_3/VC$ catalyst as well.

Table 3 $\overline{M}_n$, $\overline{M}_w$ and PDI of the PMMA side chains catalyzed with different catalysts.

Catalyst	$FeCl_2/PPh_3/VC$	CuCl/BPy
$\overline{M}_n$ (g/mol)	2,104	4,693
$\overline{M}_w$ (g/mol)	3,491	5,338
PDI	1.62	1.14

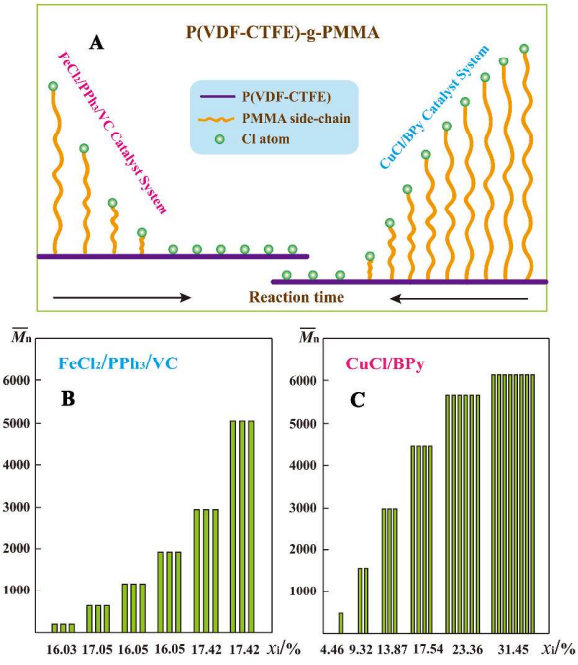

Fig. 5 Schematic illustration of the different structure of P(VDF-CTFE)-*g*-PMMA catalyzed with different catalysts.

Taking the grafting density into account, the P(VDF-CTFE)-*g*-PMMA synthesized from two catalysts could be illustrated in Fig. 5. A small amount of PMMA side chains with large length distribution are grafted onto P(VDF-CTFE) when $FeCl_2/PPh_3$/VC is utilized as catalyst. On the contrary, a great number of PMMA side-chains with more uniform chain length are formed when the polymerization is catalyzed with CuCl/BPy under the same reaction conditions (Fig. 5A). In addition, the molecular weight distribution was more concentrated obtained from CuCl/BPy catalyst (as shown in Table 2 and Fig. 5C), while much more scattered grafted polymer chains were obtained in the copolymer catalyzed with $FeCl_2/PPh_3$/VC (Table 2 and Fig.5B). That further confirmed the better controllability and higher activity of CuCl/BPy catalyst system.

3.5 Kinetic analysis of the initiation and propagation rate during the synthesis of P(VDF-CTFE)-*g*-PMMA

To understand the evolution of the polymerization deeply and correlate the structure of the copolymer to the fundamental parameters, kinetic analysis was conducted and fitted with the experimental results. The grafting polymerization of MMA initiated with P(VDF-CTFE) was divided into two steps including the initiation reaction and the propagation reaction since the reaction system possesses two kinds of active species (R-Cl and RM_n-Cl (n = 1, 2, 3…)) and their reaction kinetics constants with catalysts should be different. As shown in Scheme 4, the initiation reaction is involving the formation of initial radical R^* from redox reaction between catalysts

($MtCl_n$/L) and CTFE on P(VDF-CTFE) (marked as R-Cl) followed by the insertion of first monomer (M) onto R^* to generate RM^* and quickly chain transferred to $MtCl_{n+1}$/L to form RM-Cl. The equilibrium constant of ATRP in this stage is marked as K_{ATRP1}, which is referring to the ratio of k_{act1} divided by k_{deact1}. R_i and k_i, representing how fast the formation of RM-Cl, are the initiation rate and the initiation rate constant. The propagation reaction is starting from the activation of RM_n-Cl (n = 1, 2, 3…) to form RM_n^* followed by the insertion of monomers as well as the chain transfer reaction to $MtCl_{n+1}$/L to generate $RM_{n+1}Cl$. The equilibrium constant of ATRP in this stage is assumed to be the same for their similar structure of RM_n-Cl with different n and marked as K_{ATRP2}, which is referring to the ratio of k_{act2} divided by k_{deact2}. R_p and k_p, referring to how fast the polymer chains are growing, are the propagation rate and its rate constant.

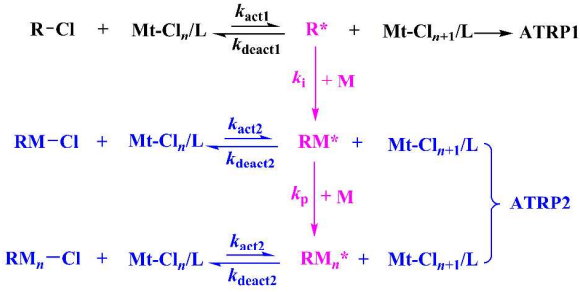

Scheme 4 The initiation and propagation reactions involving two kinds of initiator species R-Cl and RM_n-Cl. (Mt-Cl_n/L stands for $FeCl_2/PPh_3$ or CuCl/BPy).

From above discussion, it can be known that the initiation reaction is in two steps including the generation of R^* from the reduction reaction of R-Cl and the addition reaction of R^* toward monomers. Therefore, the initiation rate R_i should be dominated

by the slower one. Usually, the first step in ATRP is rather fast and the equilibrium would be established in short time. The second step is the rate controlling step and R_i could be expressed as $R_i = k_i[R^*][M]$ (red in Scheme 4). However, the activating reaction of R-Cl onto P(VDF-CTFE) in this case is rather slow as discussed above and the first step is much slower than the addition reaction of R^* to monomer. Therefore, R_i should be dominated by the first step instead of the second one and it should be defined as eq (16),

$$R_i = -\frac{d[\text{R-Cl}]}{dt} = k_{act1}[\text{R-Cl}][\text{MtCl}_n / \text{L}] \qquad \text{eq (16)}$$

From Scheme 4, the propagation rate R_p could be expressed as eq (17),

$$R_p = -\frac{d[\text{M}]}{dt} = k_p[\text{RM}^*][\text{M}] = k_p K_{\text{ATRP2}} \frac{[\text{MtCl}_n / \text{L}]}{[\text{MtCl}_{n+1} / \text{L}]}[\text{RM}_n\text{-Cl}][\text{M}] \qquad \text{eq (17)}$$

Integrating eq (16) against reaction time from 0 to t,

$\int_0^t -\frac{d[\text{R-Cl}]}{[\text{R-Cl}]} = \int_0^t k_{act1}[\text{MtCl}_n / \text{L}]dt$, then

$\ln \frac{[\text{R-Cl}]_0}{[\text{R-Cl}]_t} = k_{act1}[\text{MtCl}_n / \text{L}]t$ and

$$[\text{R-Cl}]_t = [\text{R-Cl}]_0 e^{-K_1 t} \qquad \text{eq (18)}$$

is obtained, where K_1 is equal to $k_{act1}[\text{MtCl}_n/\text{L}]$. Therefore, the initiating rate is directly correlated to the activate rate constant k_{act1} and the concentration of metal salts in reductive states reasonablely. The value of K_1 could be obtained by fitting the function $[\text{R-Cl}]_t = [\text{R-Cl}]_0 e^{-K_1 t}$ with the experimental results ($[\text{CTFE}]_t \sim t$). As shown in Fig. 6, K_1 of $FeCl_2/PPh_3$/VC and CuCl/BPy system is determined as 1/750 and 1/77, respectively, which means the initiation activity of $FeCl_2/PPh_3$/VC system to P(VDF-CTFE) is much smaller than that of CuCl/BPy system under the consistent

conditions. Because the initial concentration of metal complex ([$MtCl_n$/L]) is consistent, the dramatic difference of K_1 observed in two catalysts should be mainly induced by the different k_{act1}, namely, the reductive capabilities of metal complex toward C-Cl onto P(VDF-CTFE). Meanwhile, the initiation speed of CTFE in both cases is not sufficient high, which leaves a large quantity of CTFE units un-initiated in the resultant copolymers. Ideally, the CTFE content should be reduced to near zero in very short period at the beginning of the polymerization. That means K_1 should be sufficient high as indicated in the curve of ideal case in Fig. 6, where $K_1 = 0.3$ is taken as an instance.

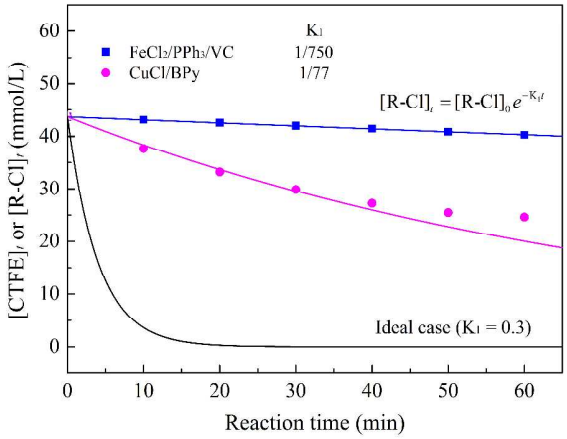

Fig. 6 Experimental and theoretical results of $[CTFE]_t$ or $[R\text{-}Cl]_t$ versus reaction time catalyzed with different catalysts.

In the propagation step, [RM_n-Cl] in the ideal living/controlled radical polymerization system is usually treated as a constant ($[R\text{-}Cl]_0$) since the structure of [R-Cl] is similar to [RM_n-Cl] and their activation energies are regarded as the same. Therefore, linear increasing trend of $\ln([M]_0/[M]_t)$ against reaction time t would be

obtained and recognized as one of the most popular utilized relationships to characterize the controlled or living nature of ATRP or other living radical polymerization since it is following the first-order kinetics. However, the concentration of propagation active sites should not be treated as a constant any longer since R-Cl and RM_n-Cl (n = 1, 2, 3…) are treated as different species in present work. Namely, the concentration of propagation active species $[RM_n\text{-Cl}]=[\text{R-Cl}]_0 - [\text{R-Cl}]_t$ is not a constant but a function of reaction time t and is obtained as $[RM_n\text{-Cl}] = [\text{R-Cl}]_0(1-e^{-K_1 t})$ based on the above discussion. Therefore, by integrating reaction time from 0 to t of eq (17), [M] as a function of time t could be observed as

$$\ln\frac{[M]_0}{[M]_t} = \int_0^t -\frac{d[M]}{[M]} = \int_0^t K_2[\text{R-Cl}]_0(1-e^{-K_1 t})dt = K_2[\text{R-Cl}]_0 t + \frac{K_2}{K_1}[\text{R-Cl}]_0(e^{-K_1 t}-1) \quad \text{eq(19)},$$

where K_2 is equal to $k_p K_{ATRP2}[MtCl_n/L]/[MtCl_{n+1}/L]$. By fitting experimental results ($\ln([M]_0/[M]_t)$ vs. t) with eq (19) as shown in Fig. 7, K_2 of CuCl/BPy and $FeCl_2/PPh_3$/VC system is obtained as 0.3 and 0.2, respectively. As indicated in $K_2=k_p K_{ATRP2}[MtCl_n/L]/[MtCl_{n+1}/L]$, the difference of K_2 between two catalyst systems is from the term of $K_{ATRP2}[MtCl_n/L]/[MtCl_{n+1}/L]$ since the addition reaction rate constant (k_p) of RM_n^* with MMA monomer should be the same. Apparently, the slightly bigger K_2 of CuCl/BPy system may be attributed to its higher redox potential than that of $FeCl_2/PPh_3$/VC system. The smaller K_1 and K_2 of $FeCl_2/PPh_3$/VC system are responsible for the lower MMA conversion and average molecular weight of PMMA grafted than CuCl/BPy catalyst.

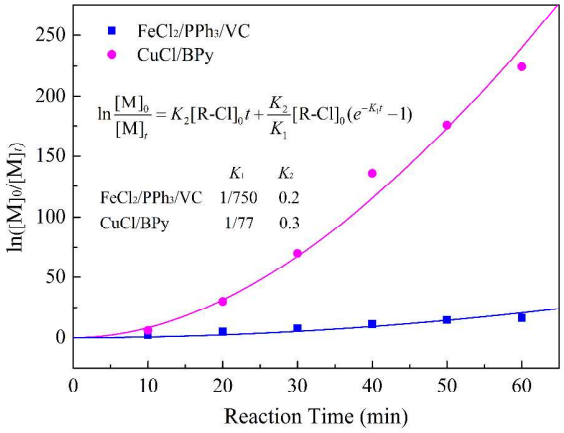

Fig. 7 Kinetic plot of $\ln([M]_0/[M]_t)$ for ATRP of MMA grafted onto P(VDF-CTFE) catalyzed with different catalysts.

Although the polymerization has been divided into two steps as shown in Scheme 4, both the catalyst and monomer are in the same concentration during the polymerization process. At the beginning, the concentration of RM_n-Cl (n = 1, 2, 3…) is zero and only initiation reaction would take place. Once the RM_n-Cl species are formed, the propagation reaction starts and the catalysts ($MtCl_n$/L) are involved in two possible reaction routes including reducing either R-Cl or RM_n-Cl species. Apparently, which one is more favorable is governed by the reductive capability of metal complex to R-Cl and RM_n-Cl species, which should be dominated by K_1 and K_2. In $FeCl_2/PPh_3$/VC system, K_1 and K_2 are 1/750 and 0.2, respectively, which means the propagation rate is over 150 times of the initiation rate when [R-Cl] and [RM_n-Cl] are the same. Apparently, the propagation reaction shows very high priority than that of initiation reaction under the consistent reaction conditions. In CuCl/BPy case, K_1 and K_2 are 1/77 and 0.3 and the propagation rate is about 23.1 times of initiation rate under the consistent conditions. The propagation reaction still shows very high

priority although it is much lower than that in $FeCl_2/PPh_3$/VC system.

In an ideal LRP system, the initiator R-Cl possessing the similar structure with growing polymer chain RM_n-Cl is usually applied in synthesizing polymer with narrow polymer distribution since K_1 is approximately equal to K_2. That means all the active species could be treated equally and activated by catalyst with the same possibility. Alternatively, high active initiators[49] whose K_1 is much bigger than that of K_2 could be utilized as well. The initiation stage takes very short time to convert all the R-Cl species into RM-Cl before the propagation of all the polymer chains starts in the exactly same rate. In both cases, the polymerization with good control/living character and resultant polymers with small PDI could be expected. However, if initiators with low activity such as P(VDF-CTFE) have to be utilized in ATRP, K_1 would be much smaller than K_2 and the high priority of propagation reaction would lead to a very poor controlling character of the polymerization together with the wide molecular weight distribution of the resultant copolymer. Apparently, the relationship of K_1 and K_2, especially the value of K_1, is playing the dominant role. The smaller of the K_1, the poorer controlling character of polymerization together with the high PDI of polymer are expected to be observed. The grafted copolymer structure is more like a block copolymer with several very long grafted copolymer chains and some very short chains together with unreacted R-Cl structure in majority as suggested in Scheme 3. In general, to obtain well controlled/living polymerization character in ATRP process, high initiation rate constant K_1 has to be ensured by increasing either the addition reaction rate constant of R^* with monomers or the reductive performance

of the metal complex catalysts if the initiator structure is reserved.

4 Conclusions

In conclusion, PMMA with different chain length and PDI were grafted onto P(VDF-CTFE) catalyzed with $FeCl_2/PPh_3$ and CuCl/BPy complexes *via* ATRP process. By removing homo-PMMA from the resultant copolymer and converting the un-initiated CTFE into TrFE units, the detailed structure information including the grafting density, average chain length, average molecular weight and its distribution of P(VDF-CTFE)-*g*-PMMA obtained from two catalysts was precisely characterized. The grafted copolymer synthesized from CuCl/BPy catalyst possesses higher grafting density, larger average molecular weight and smaller PDI than that of $FeCl_2/PPh_3$ system for its higher reductive potential. The evolution of the PMMA side chains was clearly illustrated by analyzing the structure of P(VDF-CTFE)-*g*-PMMA synthesized from two catalysts in different reaction time. By dividing the propagation reaction into two different steps for the difference of initial (R-Cl) and growing (RM_n-Cl) active species, the kinetics analysis was conducted and found to fit the experimental results very well. Two kinetics constants (K_1 and K_2) were obtained to dominate the initiation and propagation performance of ATRP process. K_1 of CuCl/BPy is about ten times larger than that of $FeCl_2/PPh_3$/VC for its relatively high reductive potential to the R-Cl species as well as the molar concentration ratio between the reductive and oxidized species. The value of K_2 obtained from two catalysts is 0.2 and 0.3, which suggests the propagation performance of two catalysts is rather close. The big difference of K_1 between two catalysts is responsible for the structure variety of the

copolymer obtained as well as the varied polymerization performance. The poor uniformity of the side chains is mostly originated from the much lower active capability of catalysts to R-Cl than that of RM_n-Cl species, namely smaller K_1 than K_2. The results may help to understand not only the detailed polymer structure synthesized from ATRP process more precisely but also the evolution of the growing polymer chains under different reaction conditions more directly.

Acknowledgments

This work was financially supported by the National Nature Science Foundation of China-NSFC (No. 10976022, 51103115, 50903065), Fundamental Research Funds for the Central Universities (xjj2013075), the National Basic Research Program of China (No. 2009CB623306), International Science & Technology Cooperation Program of China (2013DFR50470), Natural Science Basic Research Plan in Shaanxi Province of China (No. 2013JZ003).

References

1 V. M. C. Coessens, K. Matyjaszewski, *J. Chem. Educ.*, 2010, **87**, 916-919.

2 W. A. Braunecker, K. Matyjaszewski, *Prog. Polym. Sci.*, 2007, **32**, 93-146.

3 L. Bai, L. Zhang, Y. Liu, X. Pan, Z. Cheng, X. Zhu, *Polym. Chem.*, 2013, **4**, 3069-3076.

4 J. S. Wang, K. Matyjaszewski, *J. Am. Chem. Soc.*, 1995, **117**, 5614-5615.

5 M. Kato, M. Kamigaito, M. Sawamoto, T. Higashimura, *Macromolecules*, 1995, **28**, 1721-1723.

6 M. Kamigaito, T. Ando, M. Sawamoto, *Chem. Rev.*, 2001, **101**, 3689-3745.

7 M. Ouchi, T. Terashima, M. Sawamoto, *Chem. Rev.*, 2009, **109**, 4963-5050.

8 V. M. C. Coessens, T. Pintauer, K. Matyjaszewski, *Prog. Polym. Sci.*, 2001, **26**, 337-377.

9 K. Davis, K. Matyjaszewski, *Adv. Polym. Sci.*, 2002, **159**, 1-13.

10 K. Matyjaszewski, *Prog. Polym. Sci.*, 2005, **30**, 858-875.

11 N. V. Tsarevsky, K. Matyjaszewski, *Chem. Rev.*, 2007, **107**, 2270-2299.

12 F. J. Xu, K. G. Neoh, E. T. Kang, *Prog. Polym. Sci.*, 2009, **34**, 719-761.

13 Y. Ogura, T. Terashima, M. Sawamoto, *ACS Macro Lett.*, 2013, **2**, 985-989.

14 S.-H. Lee, M. Ouchi, M. Sawamoto, *Macromolecules*, 2012, **45**, 3702-3710.

15 K. Nakatani, Y. Ogura, Y. Koda, T. Terashima, M. Sawamoto, *J. Am. Chem. Soc.*, 2012, **134**, 4373-4383.

16 T. Terashima, A, Nomura, M. Ito, M. Ouchi, M. Sawamoto, *Angew. Chem. Int. Ed.*, 2011, **50**, 7892-7895.

17 W. Jakubowski, K. Matyjaszewski, *Macromolecules*, 2005, **38**, 4139-4146.

18 S. Qin, J. Saget, J. Pyun, S. Jia, T. Kowalewski, K. Matyjaszewski, *Macromolecules*, 2003, **36**, 8969-8977.

19 D. Neugebauer, M. Theis, T. Pakula, G. Wegner, K. Matyjaszewski, *Macromolecules*, 2006, **39**, 584-593.

20 B. Dufour, C. Tang, K. Koynov, Y. Zhang, T. Pakula, K. Matyjaszewski, *Macromolecules*, 2008, **41**, 2451-2458.

21 M. Li, N. M. Jahed, K. Min, K. Matyjaszewski, *Macromolecules*, 2004, **37**, 2434-2441.

22 Y. Miura, K. Satoh, M. Kamigaito, Y. Okamoto, T. Kaneko, H. Jinnai, S. Kobukata, *Macromolecules*, 2007, **40**, 465-473.

23 H.-I. Lee, K. Matyjaszewski, S. Yu, S. S. Sheiko, *Macromolecules*, 2005, **38**, 8264-8271.

24 V. Percec, B. Barboiu, C. Grigoras, T. K. Bera, *J. Am. Chem. Soc.*, 2003, **125**, 6503-6516.

25 K. T. Powell, C. Cheng, K. L. Wooley, *Macromolecules*, 2007, **40**, 4509-4515.

26 W. Tang, Y. Kwak, W. Braunecker, N. V. Tsarevsky, M. L. Coote, K. Matyjaszewski, *J. Am. Chem. Soc.*, 2008, **130**, 10702-10731.

27 Y. Zhang, Y. Wang, K. Matyjaszewski, *Macromolecules*, 2011, **44**, 683-685.

28 B. Ameduri, B. Boutevin, G. Kostov, *Prog. Polym. Sci.*, 2001, **26**, 105−187.

29 B. Ameduri, *Macromolecules*, 2010, **43**, 10163-10184.

30 K. Johns, G. Stead, *J. Fluorine Chem.*, 2000, **104**, 5-18.

31 L. Q. Xu, J. C. Chen, R. Wang, K.-G. Neoh, E.-T. Kang, G. D. Fu, *RSC. Adv.*, 2013, **3**, 25204-25214.

32 R. Chan, V. Chen, *J. Membr. Sci.*, 2004, **242**, 169-188.

33 L. Yan, Y. S. Li, C. B. Xiang, *Polymer*, 2005, **46**, 7701-7706.

34 Y. H. Zhao, Y. L. Qian, B. K. Zhu, Y. Y. Xu, *J. Membr. Sci.*, 2008, **310**, 567-576.

35 M. F. Zhang, T. P. Russell, *Macromolecules*, 2006, **39**, 3531-3539.

36 F. He, B. W. Luo, S. J. Yuan, B. Liang, C. Choong, S. O. Pehkonenc, *RSC Adv*, 2014, **4**, 105-117.

37 S, Samanta, D. P. Chatterjee, S. Manna, A. Mandal, A. Garai, A. K. Nandi, *Macromolecules*, 2009, **42**, 3112-3120.

38 F. X. Guan, Z. Z. Yuan, E. W. Shu, L. Zhu, *Appl. Phys. Lett.*, 2009, **94**, 052907.

39 F. X. Guan, L. Y. Yang, J. Wang, B. Guan, K. Han, Q. Wang, L. Zhu, *Adv. Funct. Mater.*, 2011, **21**, 3176-3188.

40 F. X. Guan, J. Wang, L. Y. Yang, J.-K. Tseng, K. Han, Q. Wang, L. Zhu, *Macromolecules*, 2011, **44**, 2190-2199.

41 L. Y. Yang, E. Allahyarov, F. X. Guan, L. Zhu, *Macromolecules*, 2013, **46**, 9698-9711.

42 E. M. W. Tsang, Z. B. Zhang, Z. Q. Shi, T. Soboleva, S. Holdcrof, *J. Am. Chem. Soc.*, 2007, **129**, 15106-15107.

43 Z. C. Zhang, E. Chalkova, M. Fedkin, C. M. Wang, S. N. Lvov, S. Komarneni, T. C. M. Chung, *Macromolecules*, 2008, **41**, 9130-9139.

44 J. J. Li, S. B. Tan, S. J. Ding, H. Y. Li, L. J. Yang, Z. C. Zhang, *J. Mater. Chem.*,

2012, **22**, 23468-23476.

45 J. J. Li, X. Hu, G. X. Gao, S. J. Ding, H. Y. Li, L. J. Yang, Z. C. Zhang, *J. Mater. Chem. C*, 2013, **1**, 1111-1121.

46 Y. Y. Lu, J. Claude, Q. M. Zhang, Q. Wang, *Macromolecules*, 2006, **39**, 6962-6968.

47 Y. Y. Lu, J. Claude, B. Neese, Q. M. Zhang, Q. Wang, *J. Am. Chem. Soc.*, 2006, **128**, 8120-8121.

48 Z. M. Wang, Z. C. Zhang, T. C. M. Chung, *Macromolecules*, 2006, **39**, 4268-4271.

49 X. Y. Zhang, C. K. Fu, , L. Feng Y. Ji, L. Tao, Q. Huang, S. X. Li, Y. Wei, *Polymer*, 2012, **53**, 3178-3184.

Figure captions

Scheme 1 Traditional ATRP mechanism.

Scheme 2 Schematic illustration of the synthesis and hydrogenation process of P(VDF-CTFE)-*g*-PMMA copolymer.

Scheme 3 Structure evolution of grafted copolymers synthesized from ATRP process. (A, Ideal case; B, Real case).

Scheme 4 The initiation and propagation reactions involving two kinds of initiator species R-Cl and RM_n-Cl. (Mt-Cl_n/L stands for $FeCl_2/PPh_3$ or CuCl/BPy).

Fig. 1 ^1H NMR spectra of (A) Pristine P(VDF-CTFE) and (B) P(VDF-CTFE)-*g*-PMMA.

Fig. 2 ^1H NMR spectra of (A) P(VDF-CTFE), (B) P(VDF-TrFE), (C) P(VDF-CTFE)-*g*-PMMA and (D) P(VDF-TrFE)-*g*-PMMA.

Fig. 3 MMA grafted (%) and CTFE activated (%) in the P(VDF-CTFE)-*g*-PMMA calculated from eq (2) and eq (5) catalyzed with $FeCl_2/PPh_3$/VC.

Fig. 4 Molar number of initiated CTFE versus reaction time during ATRP process catalyzed with $FeCl_2/PPh_3$/VC and CuCl/BPy.

Fig. 5 Schematic illustration of the different structure of P(VDF-CTFE)-*g*-PMMA catalyzed with different catalysts.

Fig. 6 Experimental and theoretical results of $[CTFE]_t$ or $[R\text{-}Cl]_t$ versus reaction time catalyzed with different catalysts.

Fig. 7 Kinetic plot of $\ln([M]_0/[M]_t)$ for ATRP of MMA grafted on P(VDF-CTFE) catalyzed with different catalysts.